



# The synthesis and biological evaluation of nucleobases/tetrazole hybrid compounds: A new class of phosphodiesterase type 3 (PDE3) inhibitors

Mohsen Shekouhy<sup>a,\*</sup>, Somaye Karimian<sup>b</sup>, Ali Moaddeli<sup>a,c</sup>, Zeinab Faghieh<sup>d</sup>, Yousef Delshad<sup>a</sup>, Ali Khalafi-Nezhad<sup>a,\*</sup>

<sup>a</sup> Department of Chemistry, College of Sciences, Shiraz University, Shiraz 71454, Iran

<sup>b</sup> Department of Medicinal Chemistry, School of Pharmacy, Shiraz University of Medical Sciences, Shiraz, Iran

<sup>c</sup> Legal Medicine Research Center, Legal Medicine Organization, Tehran, Iran

<sup>d</sup> Pharmaceutical Sciences Research Center, Shiraz University of Medical Sciences, Shiraz, Iran

## ARTICLE INFO

### Keywords:

Cilostazol  
Phosphodiesterase  
Nucleobase/tetrazole hybrid  
HeLa cell line  
MCF-7 cell line

## ABSTRACT

Inspired by the chemical structure of Cilostazol, a selective phosphodiesterase 3A (PDE3A) inhibitor, several novel hybrid compounds of nucleobases (uracil, 6-azauracil, 2-thiuracil, adenine, guanine, theophylline and theobromine) and tetrazole were designed and successfully synthesized and their inhibitory effects on PDE3A as well as their cytotoxicity on HeLa and MCF-7 cancerous cell lines were studied. Obtained results show the linear correlation between the inhibitory effect of synthesized compounds and their cytotoxicity. In some cases, the PDE3A inhibitory effects of synthesized compounds are higher than the Cilostazol. Besides, compared to a standard anticancer drug methotrexate, some of the synthesized compounds showed the higher cytotoxicity against the HeLa and MCF-7 cancerous cell lines.

## 1. Introduction

So far, eleven cyclic nucleotide phosphodiesterase gene families (PDE1-11) have been identified in different cells and tissues. All types of phosphodiesterases (PDEs) have unique characteristics such as primary amino acid sequences in their structures, sensitivity to specific inhibitors, affinities for cyclic adenosine monophosphate (cAMP) and cyclic guanosine monophosphate (cGMP) and their biological regulatory pathways.<sup>1-11</sup> The influence of PDEs on different disease pathogenesis and their potency as new therapeutic targets have been studied and proven.<sup>12</sup> It is well proven that the overexpression of PDEs which results in impaired cAMP and cGMP generation happens in various cancer cells.<sup>13</sup> The regulation of tumor microenvironment with the selective inhibition of PDEs which raises the level of intracellular cAMP and cGMP will lead to the induction of apoptosis and the cell cycle arresting. So, the development and application of new specific inhibitors of PDEs which regulate the intracellular signaling may lead to the opening of a gateway to the novel therapeutic drugs for cancer with reduced adverse effects.<sup>14,15</sup> Recent studies on the inhibitors of phosphodiesterase type 3 (PDE3) indicate the important role of this enzyme in the regulation of cAMP-modulated processes such as platelet aggregation, myocardial contractility and antipolytic action.<sup>1-3</sup> As the overexpression of PDE3 in cancer cells is recently well-proven, the

inhibition of this enzyme along with the other types of PDE may lead to the inhibition of tumor growth and angiogenesis.<sup>16-20</sup>

Nucleobases are an important group of nitrogen heterocycles with unique biological activities. These compounds are the main building blocks of DNA and RNA and play different roles in numerous important biological processes.<sup>21,22</sup> These unique characteristics lead to the use of nucleobases as pharmacophores in medicinal chemical research, especially as anticancer agents.<sup>23-25</sup> Nowadays, a broad range of clinically applied anticancer agents are modified nucleobases and there are many other reports about the potent cytotoxicity of these compounds against the cancerous cell lines *in vitro* through different mechanisms.<sup>25</sup>

Cilostazol is a phosphodiesterase type 3 (PDE3) inhibitor with a therapeutic focus on cyclic adenosine monophosphate (cAMP). It inhibits platelet aggregation and is a direct arterial vasodilator. Its main effects are dilation of the arteries supplying blood to the legs and decreasing platelet coagulation.<sup>26</sup> The chemical structure of Cilostazol consists of a tetrazole/quinolinone hybrid (Fig. 1).

Considering the above-mentioned facts about the potency of PDE3 inhibitors as anticancer agents and the widespread application of modified nucleobases for cancer treatment and inspired by the chemical structure of Cilostazol as a PDE3 inhibitor, we herein present the synthesis, PDE3 inhibitory and anticancer properties of some novel nucleobases/tetrazole hybrids.

\* Corresponding authors.

E-mail addresses: [m.shekouhy@shirazu.ac.ir](mailto:m.shekouhy@shirazu.ac.ir) (M. Shekouhy), [khalafi@shirazu.ac.ir](mailto:khalafi@shirazu.ac.ir) (A. Khalafi-Nezhad).

<https://doi.org/10.1016/j.bmc.2020.115540>

Received 16 January 2020; Received in revised form 22 April 2020; Accepted 29 April 2020

Available online 05 May 2020

0968-0896/ © 2020 Elsevier Ltd. All rights reserved.

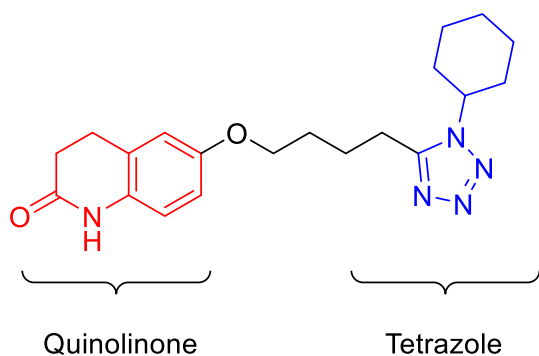


Fig. 1. The chemical structure of Cilostazol as a clinically used PDE3 inhibitor.

## 2. Results and discussions

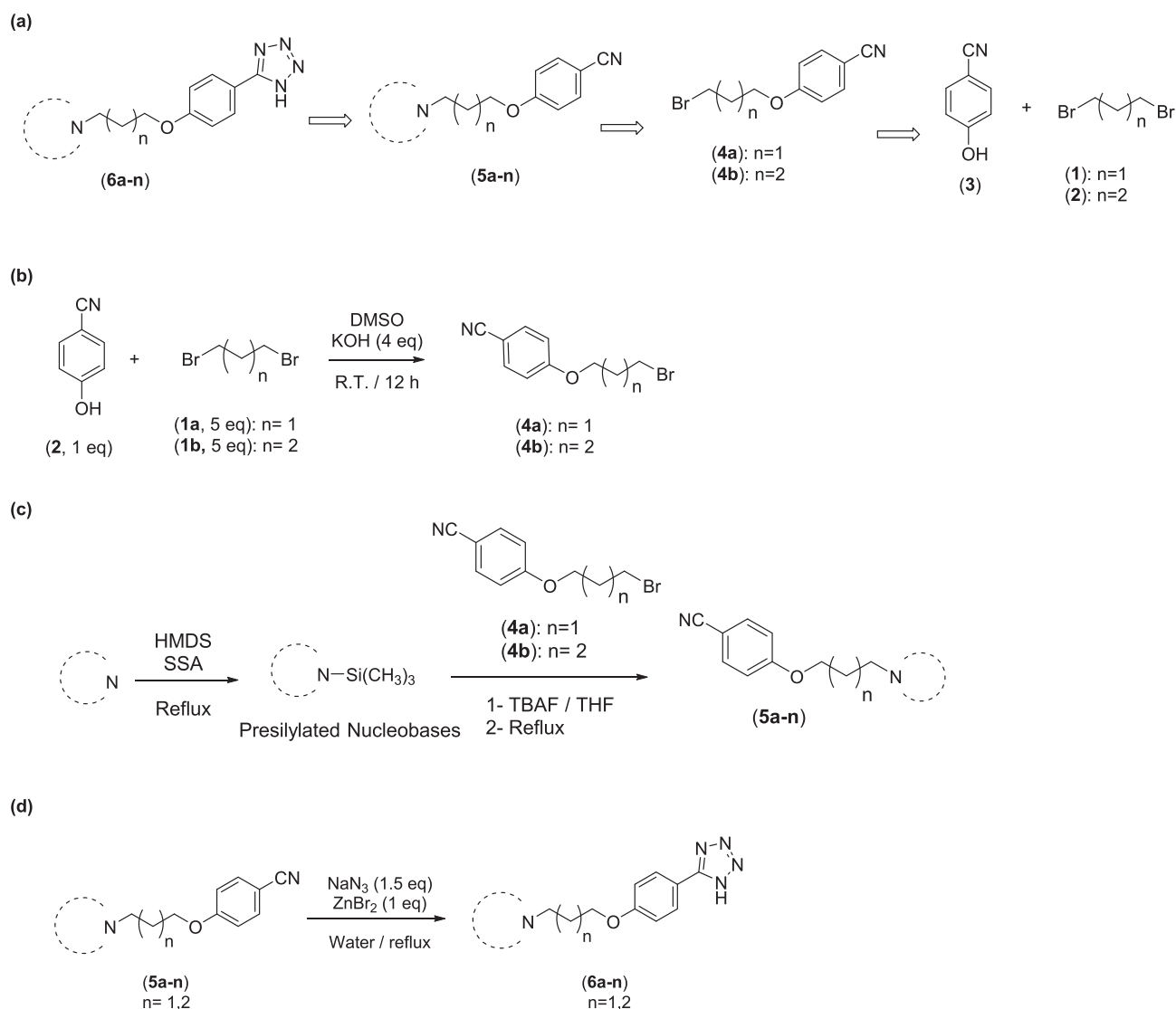
### 2.1. Chemistry

Our primary retrosynthetic approach for the preparation of nucleobase-contained hybrid compounds of tetrazole is summarized in Scheme 1a. According to this retrosynthesis pathway, the key

intermediates are compounds (5a-n). Thus, our study started with the production of compounds (5a-n). These molecules are easily obtained from the reaction of nucleobases with nitriles (4a and 4b). To prepare nitriles (4a and 4b), 4-hydroxybenzonitrile (3) was treated with 1,3-dibromopropane (1) or 1,4-dibromobutane (2).

At first, 4-(3-bromopropoxy)benzonitrile (4a) and 4-(4-bromobutoxy)benzonitrile (4b) were synthesized with the reaction of 4-hydroxybenzonitrile (3) and excess amounts of 1,3-dibromopropane (1) or 1,3-dibromobutane (2) respectively, in DMSO in the presence of KOH at room temperature (Scheme 1b).<sup>27</sup>

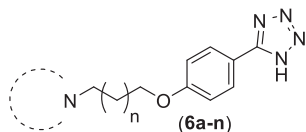
In the next step, nucleobases were presilylated according to a reported procedure<sup>28</sup> and then were added nucleophilically to 4-(3-bromopropoxy)benzonitrile (4a) and 4-(4-bromobutoxy)benzonitrile (4b) to gain the nucleobase-contained nitriles (5a-n) as key intermediates for the synthesis of nucleobase-contained tetrazoles (6a-n) (Scheme 1c). The presilylation step was done to improve the solubility as well as regioselectivity during the nucleophilic addition of nucleobases to nitriles (5a) and (5b).<sup>28</sup> Using this method, various pyrimidine nucleobases such as uracil, 6-azauracil and 2-thiouracil as well as purine nucleobases such as adenine, guanine, theophylline and theobromine were successfully applied and corresponding nucleobase-contained nitriles (5a-n) were obtained in very good yields (69–89%).



Scheme 1. a. (a) The retrosynthetic analysis of the designed nucleobase-contained hybrid compounds of tetrazole (6a-n), (b) The preparation of nitriles (4a) and (4b), (c) The preparation of nucleobase-contained nitriles (5a-n), (d) The preparation of nucleobase-contained hybrid compounds of tetrazoles (6a-n).

**Table 1**

The preparation of nucleobase-contained hybrid compounds of tetrazoles (**6a-n**) with the reaction of nucleobase-contained nitriles (**5a-n**) and  $\text{NaN}_3$  in the presence of  $\text{ZnBr}_2$  in the water at reflux temperature.



Entry	n	Nucleobase	Product	Yield (%) <sup>a</sup>	M.P. (°C)
2	1	6-Azauracil	<b>6b</b>	86	212–213
3	1	2-Thiouracil	<b>6c</b>	88	170–172
4	1	Adenine	<b>6d</b>	85	229–231
5	1	Guanine	<b>6e</b>	89	221–223
6	1	Theophylline	<b>6f</b>	88	238–241
7	1	Theobromine	<b>6g</b>	85	219–222
8	2	Uracil	<b>6h</b>	87	208–210
9	2	6-Azauracil	<b>6i</b>	83	212–214
10	2	2-Thiouracil	<b>6j</b>	86	185–188
11	2	Adenine	<b>6k</b>	89	216–218
12	2	Guanine	<b>6l</b>	87	225–227
13	2	Theophylline	<b>6m</b>	85	200–203
14	2	Theobromine	<b>6n</b>	85	220–223

<sup>a</sup> Isolated pure products

Please note that in the case of adenine, guanine, and theophylline the alkylation process will occur on the nitrogen number 9, 9 and 7 respectively that are placed on the five-membered ring, but in the case of theobromine, the alkylation process will occur on the nitrogen number 1 that is placed on the six-membered ring of theobromine.

In order to the preparation of nucleobase-contained hybrids of tetrazoles (**6a-n**), synthesized nucleobase-contained nitriles (**5a-n**) were reacted with  $\text{NaN}_3$  using a reported procedure by Sharpless *et al.*<sup>29</sup> For this, a mixture of nucleobase-contained nitriles (**5a-n**, 1 eq) and  $\text{NaN}_3$  (1.5 eq) was refluxed in water in the presence of  $\text{ZnBr}_2$  (1 eq) for 24 h (Scheme 1d) and obtained results are summarized in Table 1. As it is shown in Table 1, using this method, all synthesized purine, as well as pyrimidine nucleobase-contained nitriles (**5a-n**), were successfully converted to their corresponding nucleobase-contained tetrazole hybrid compounds (**6a-n**).

## 2.2. Biology

After successful synthesis of target nucleobase/tetrazole hybrid compounds (**6a-n**) their cytotoxicity against HeLa and MCF-7 cell lines were studied by MTT assay. Moreover, the inhibitory effect of synthesized compounds against the PDE3A was analyzed using an IMAP TR-FRET phosphodiesterase assay kit with the use of cAMP as a substrate and obtained results were summarized in Table 2. By drawing a graph of the cytotoxicity against the inhibitory effect of synthesized compounds, it turns out that there is a direct relationship ( $R^2 = 0.98$ ) between these two factors (Fig. 1).

According to the summarized data in Table 2, compounds (**6d**) (Table 2, entry 4), (**6e**) (Table 2, entry 5) and (**6h**) (Table 2, entry 8) are more strong inhibitors of PDE3A than the Cilostazol. Between these compounds, compound (**6e**) is the strongest PDE3A inhibitor. Moreover, the most cytotoxic compounds against both HeLa and MCF-7 cell lines are (**6d**), (**6e**) and (**6h**) and the most cytotoxic compound is (**6e**). Also, it is important to mention that, compounds (**6d**), (**6e**) and (**6h**) showed a better growth inhibitory effect than the well-known anticancer drug methotrexate with  $\text{IC}_{50}$  values of  $27.94 \pm 0.36 \mu\text{M}$  and  $49.22 \pm 1.01 \mu\text{M}$  against HeLa and MCF-7 cell lines respectively. By comparing the cytotoxicity with that of the well-known anticancer drug methotrexate, we found that the synthesized compounds (**6d**), (**6e**) and

**Table 2**

The cytotoxicity and inhibitory effect of synthesized nucleobase/tetrazole hybrid compounds (**6a-n**) on HeLa and MCF-7 cell lines and PDE3A.

Entry	Compound	Growth inhibition $\text{IC}_{50}$ ( $\mu\text{M}$ ) $\pm$ SEM		PDE3 inhibition $\text{IC}_{50}$ (nM) $\pm$ SEM
		HeLa	MCF-7	
1	<b>6a</b>	$38.86 \pm 2.33$	$54.01 \pm 1.21$	$4.00 \pm 1.01$
2	<b>6b</b>	$49.31 \pm 3.14$	$65.58 \pm 2.33$	$5.08 \pm 0.34$
3	<b>6c</b>	$57.66 \pm 4.26$	$80.72 \pm 4.41$	$6.22 \pm 1.03$
4	<b>6d</b>	$21.12 \pm 2.13$	$29.35 \pm 1.86$	$2.17 \pm 0.37$
5	<b>6e</b>	$18.37 \pm 2.47$	$25.71 \pm 3.85$	$1.89 \pm 0.75$
6	<b>6f</b>	$55.33 \pm 3.10$	$74.69 \pm 2.63$	$5.83 \pm 1.02$
7	<b>6g</b>	$61.06 \pm 1.36$	$73.27 \pm 4.12$	$6.29 \pm 0.57$
8	<b>6h</b>	$25.56 \pm 2.85$	$35.78 \pm 3.22$	$2.41 \pm 1.12$
9	<b>6i</b>	$63.31 \pm 3.13$	$75.97 \pm 2.60$	$6.78 \pm 1.21$
10	<b>6j</b>	$50.65 \pm 2.45$	$68.37 \pm 1.68$	$5.13 \pm 1.05$
11	<b>6k</b>	$38.35 \pm 2.13$	$54.45 \pm 4.43$	$3.91 \pm 1.06$
12	<b>6l</b>	$68.01 \pm 2.82$	$90.45 \pm 6.25$	$7.15 \pm 0.78$
13	<b>6m</b>	$45.06 \pm 2.24$	$59.47 \pm 3.26$	$4.74 \pm 1.06$
14	<b>6n</b>	$59.91 \pm 1.16$	$73.68 \pm 2.04$	$6.50 \pm 1.11$
15	Cilostazol	–	–	$3.89 \pm 2.02$
16	Methotrexate	$27.94 \pm 0.36$	$49.22 \pm 1.01$	–

(**6h**) showed excellent activity in both breast cancer (MCF-7) and cervical cancer cell lines (HeLa).

As it was mentioned in the introduction section, the inhibition of PDEs may lead to the death of cancer cells. The linear correlation between the PDE3A inhibitory effects of synthesized compounds and their cytotoxicity could be a reason to prove that synthesized compounds kill the cancer cells by inhibiting the PDE3A activity. As it can be concluded from the summarized data in Table 2, when the nucleobases were connected to the tetrazole moiety with a propyl group, the presence of guanine and adenine (two purine-like nucleobases) in the final structure of synthesized hybrid compound provide the strongest inhibitory effect against the PDE3A as well as the highest cytotoxicity against the HeLa and MCF-7 cell lines (Table 2, entries 4 and 5). Whereas, when the nucleobases were connected to the tetrazole moiety with a butyl group, the presence of uracil (a pyrimidine-like nucleobase) in the final structure of synthesized hybrid compound provide the strongest inhibitory effect against the PDE3A as well as the highest cytotoxicity against the HeLa and MCF-7 cell lines (Table 2, entry 8).

## 2.3. Docking studies

We also performed docking studies parallel to the synthesis and *in vitro* evaluation of compounds to gain a more exhaustive conception of the interactions and binding to the PDE3A enzyme. The correctness of the docking method was checked by calculating the correlation between theoretical  $K_i$  (Table 3) and the experimental  $\text{IC}_{50}$  of the synthesized compounds against the PDE3A (Table 2). A high correlation between theoretical  $K_i$  and  $\text{IC}_{50}$  values of synthesized hybrid compounds against the PDE3A has been considered to be proof of the efficacy of the docking procedure (Fig. 2).

Molecular docking results of fourteen synthesized compounds were compared with the standard ligand, that is, Cilostazol (Table 3). The lower values of interaction energies indicated the more stable complex formed between the ligand and target enzyme. Docking data indicate that the compound (**6e**) scored more than any other compounds which is consistent with experiments and comparable with the standard ligand. Protein-ligand interactions of compound (**6e**) display favorable H-bond interactions that are highly similar to the Cilostazol. The most important interactions between the synthesized compounds and the PDE3A are the purine-<sup>2</sup>NH interaction with Asp26, carbonyl 'O' of purine ring with His58 and tetrazole-H with Gln190 (albeit Gln190 is a key residue in hydrogen bond formation because all the represented compounds (except compound **6l**) have at least one hydrogen bond through this residue). Moreover, purine-<sup>7</sup>NH interacts with His29 and

**Table 3**

The docking results of the synthesized nucleobase/tetrazole hybrids into the PDE3A binding site. (PDB ID:1LRC).

Entry	Ligand	Lowest Binding Energy (Kcal/mol)	Protein-Ligand Interactions <sup>a</sup>	Ki ( $\mu$ M) in silico
1	<b>6a</b>	-9.06	<b>Gln190, Asp139, Asn141</b> , Pro143, Phe178, Ile157, Leu189, Trp153	91.88
2	<b>6b</b>	-8.88	<b>Gln190, Asp139, Ala138</b> , Phe193, Trp153, Phe178, Ile157, Phe161	124.39
3	<b>6c</b>	-8.30	<b>Gln190, Asp139, Asn141</b> , Phe193, Ile157, Trp153, Phe161, Phe178, Leu189	244.09
4	<b>6d</b>	-9.62	<b>Gln190, Asp26, Asp139, Asn141, Gly142</b> , Trp153, Ile157, Pro143, Ala138	35.70
5	<b>6e</b>	-9.74	<b>Gln190, Asp26, His58, His29, Asp139</b> , Ile157, His150, Pro143	24.94
6	<b>6f</b>	-8.32	<b>Gln190, Asp139, Asn141</b> , Phe193, Ile157, Trp153, Pro143, Phe161, Phe178, Leu189	244.09
7	<b>6g</b>	-8.30	<b>Gln190, Asp139, Asn141, Phe193, Ile157, Trp153, Phe161, Phe178, Leu99</b>	272.31
8	<b>6h</b>	-9.34	<b>Gln190, Thr154, Ser192</b> , Phe193, Ile157, Pro143, His150, Ser192	61.08
9	<b>6i</b>	-8.07	<b>Gln190, Ser176, Ile157, Met179, Ala35, Thr33, Pro177, Phe161</b>	480.21
10	<b>6j</b>	-8.35	<b>Gln190, Asp139, Asn141</b> , Phe193, Ile157, Trp153, Pro143, Phe161, Phe178, Leu189	300.66
11	<b>6k</b>	-8.85	<b>Gln190, Asp139, Asn141, Ile157, Trp153, Phe161, Phe178, Leu189</b>	129.36
12	<b>6l</b>	-7.98	<b>Asp26, Asp139, Ile157, Trp153, Pro143</b>	568.38
13	<b>6m</b>	-8.55	<b>Gln190, Asp139, Asn141, Phe193, Ile157, Ile197, Pro143</b>	219.34
14	<b>6n</b>	-8.26	<b>Gln190, Thr154, Asp139, Ile140, Pro143, His150</b>	343.21
15	Cilostazol	-8.73	<b>Gln190, Asp26, His58</b> , Phe193, Ile157, Pro143, His150, leu99	157.66

<sup>a</sup> Amino acid residues in bold represents H-bond interactions, and the rest are  $\pi$ - $\pi$ , alkyl- $\pi$ , van der Waals and  $\pi$ -anion interactions.

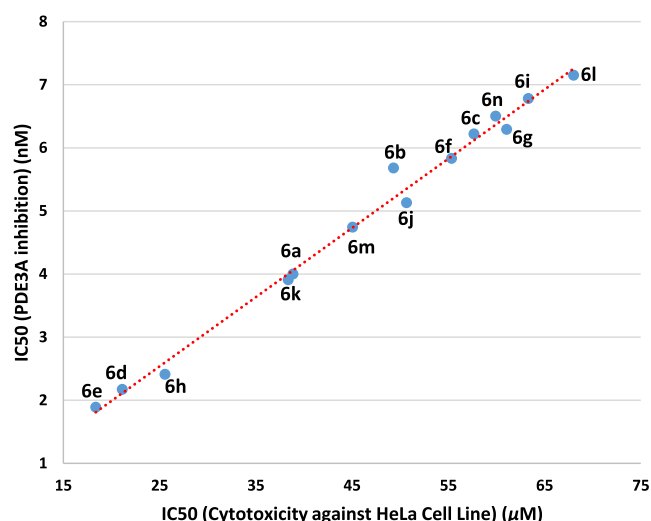


Fig. 2. The correlation between PDE3A inhibition and cytotoxicity of synthesized nucleobase/tetrazole hybrid compounds (6a-n) on the HeLa cell line.

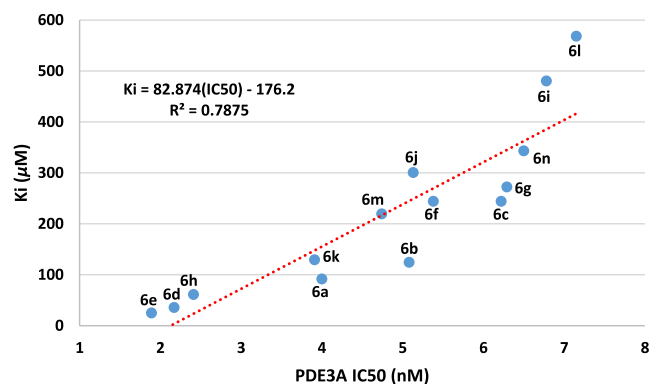


Fig. 3. The correlation between theoretical calculated Ki and experimental IC<sub>50</sub> in PDE3A.

purine-<sup>2</sup>NH interacts with Asp139 (Fig. 3). There are a few greasy amino acids, like Ile157, Pro143, Phe193, Phe161, Phe178, Leu189 and Trp153 at the binding site, so this can provide an opportunity for hydrophobic interactions with synthesized compounds (Table 3). Summarized results of molecular docking and summary of protein-ligand interactions of synthesized compounds are shown in Table 3 (see Fig. 4).

### 3. Conclusion

In conclusion, spired by the chemical structure of Cilostazol, a selective phosphodiesterase 3A (PDE3A) inhibitor, fourteen novel hybrid compounds of nucleobases (uracil, 6-azauracil, 2-thiuracil, adenine, guanine, theophylline and theobromine) and tetrazole were designed, successfully synthesized and characterized by various spectral and analytical techniques. All synthesized compounds showed the inhibitory effect against the PDE3A and in some cases the synthesized compounds (compounds (6d), (6e) and (6h)) inhibit the PDE3A stronger than the Cilostazol. The *in vitro* activity of all synthesized compounds has been evaluated against the HeLa human cervical cancer and MCF-7 human breast cancer cell lines and compared with methotrexate, a well-known anticancer agent. Based on the obtained results, the cytotoxicity of compounds (6d), (6e) and (6h) against both applied cancerous cell lines was higher than methotrexate. The docking data indicate that the compound (6e) scored more than any other compounds which is consistent with experiments and comparable. Protein-ligand interactions of compound (6e) display favorable H-bond interactions that are highly similar to the Cilostazol. The most important interactions between the synthesized compounds and the PDE3A are the purine-<sup>2</sup>NH interaction with Asp26, carbonyl 'O' of purine ring with His58 and tetrazole-H with Gln190. Moreover, purine-<sup>7</sup>NH interacts with His29 and purine-<sup>2</sup>NH interacts with Asp139. There are a few greasy amino acids, like Ile157, Pro143, Phe193, Phe161, Phe178, Leu189 and Trp153 at the binding site, so this can provide an opportunity for hydrophobic interactions with synthesized compounds. There is a direct relationship ( $R^2 = 0.98$ ) between the cytotoxicity and PDE3A inhibitory effects of synthesized compounds which could be evidence that the synthesized compounds kill the cancer cells by inhibiting the PDE3A activity.

### 4. Experimental

#### 4.1. Chemistry

All reagents and solvents were purchased from Merck, Fluka or Sigma-Aldrich. Melting points were determined in capillary tubes in a Büchi B-545 apparatus. IR spectroscopy (Shimadzu FT-IR 8300 spectrophotometer) in  $\text{cm}^{-1}$ , was employed for characterization of the compounds. Mass spectra were recorded on an Agilent GC-Mass apparatus. The reaction monitoring was accomplished by TLC on silica gel PolyGram SILG/UV254 plates. Column chromatography was carried out on columns of silica gel 60 (70–230 mesh). The eluent solvents were petroleum ether, ethyl acetate or mixture of these. Solvents for chromatography were purified by distillation before use. The <sup>1</sup>H NMR

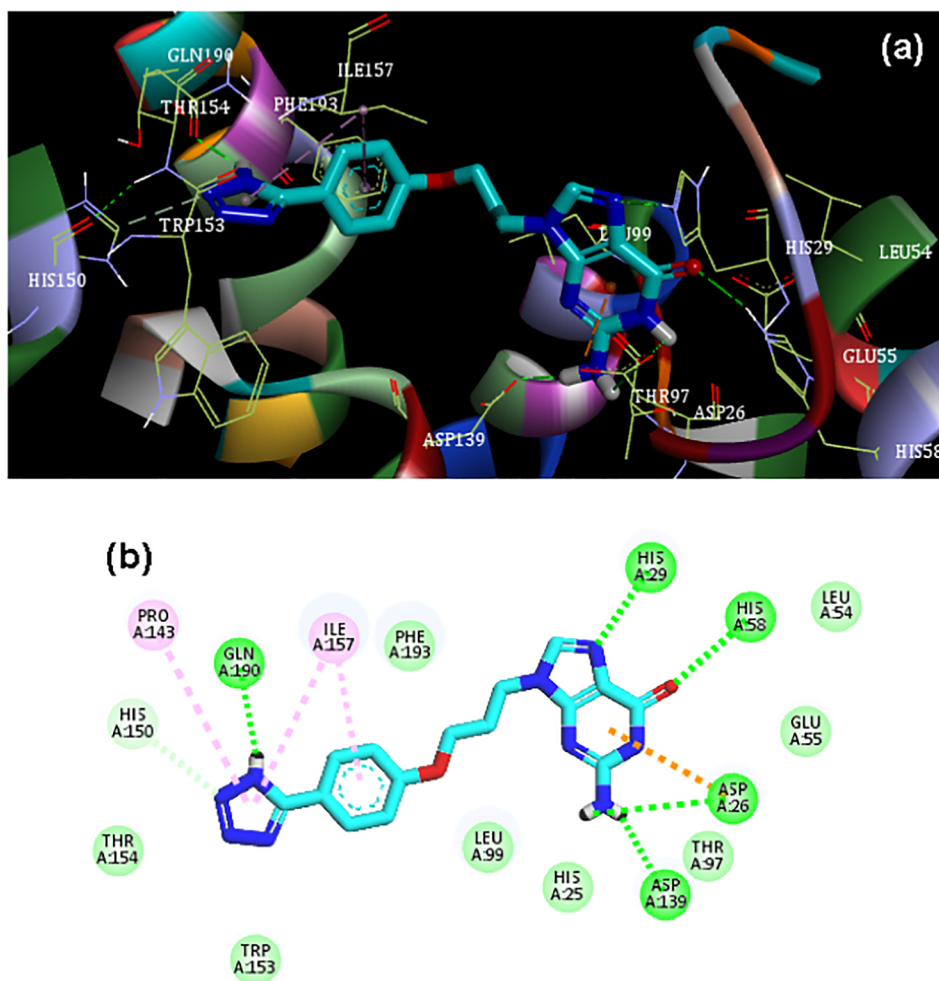


**Fig. 4.** (a) The binding orientation and (b) interactions of compound (**6e**) into the PDE3A enzyme. Ligand (**6e**) is displayed as cyan sticks, while the core amino acid residues are shown as olive sticks. Hydrogen bonding, alkyl- $\pi$ , van der Waals and  $\pi$ -anion interactions are displayed as green, pink, emerald, and apricot, respectively.

(250 MHz) and  $^{13}\text{C}$  NMR (62.5 MHz) were run on a Bruker Avance DPX-250 fourier transform (FT)-NMR spectrometer. Chemical shifts are given as  $\delta$  values against tetramethylsilane (TMS) as the internal standard and  $J$  values are given in Hz. The elemental analysis was performed on a Perkin-Elmer 240-B microanalyzer.

#### 4.1.1. The preparation of 4-(3-bromopropoxy)benzonitrile (**4a**) and 4-(4-bromobutoxy)benzonitrile (**4b**)

In a 250 mL round bottom flask containing DMSO (100 mL), powdered KOH (200 mmol, 11.2 g) was added. After stirring for 10 min, 4-hydroxybenzonitrile (50 mmol, 5.9 g) was added followed immediately by 1, $n$ -dibromo alkanes [ $n = 3,4$ ] (250 mmol,  $n = 3$ : 25.3 mL,  $n = 4$ : 29.8 mL) and stirring was continued for 12 h at room temperature. After this time. The mixture was poured into the water (1000 mL) and extracted with dichloromethane ( $3 \times 200$  mL), the combined organic extract were washed with water ( $5 \times 100$  mL) and dried under  $\text{Na}_2\text{SO}_4$  and the solvent was evaporated. The crudes were purified by column chromatography on silica gel eluting with a proper solvent ( $n$ -hexane until the separation of excess 1, $n$ -dibromo alkanes and then a mixture of  $n$ -hexane/EtOAc 4:1) and the products were obtained in 78% yields.

**4.1.1.1. 4-(3-Bromopropoxy)benzonitrile (**4a**).** Yellow oil, Purified with column chromatography using  $n$ -hexane/EtOAc 4:1 as an eluent,  $R_f = 0.59$ .  $\nu_{\text{max}}$  (KBr) 837, 1103, 1284, 1438, 1508, 1585, 2233, 2935, 3047  $\text{cm}^{-1}$ .  $^1\text{H}$  NMR (250 MHz,  $\text{CDCl}_3$ ):  $\delta$  (ppm) 2.26 (m, 2H), 3.28 (t,  $J = 6.2$  Hz, 2H), 3.94 (t,  $J = 6.2$ , 2H), 6.86 (d,  $J = 8.3$  Hz, 2H),

7.60 (d,  $J = 8.3$  Hz, 2H).  $^{13}\text{C}$  NMR (62.5 MHz,  $\text{CDCl}_3$ ):  $\delta$  (ppm) 28.9, 31.4, 66.1, 103.2, 114.1, 117.8, 132.7, 158.8. Anal. Calcd for  $\text{C}_{10}\text{H}_{10}\text{BrNO}$ : C, 50.02; H, 4.20; N, 5.83%. Found: C, 50.12; H, 4.12; N, 5.95%.

**4.1.1.2. 4-(4-Bromobutoxy)benzonitrile (**4b**).** Yellow oil, Purified with column chromatography using  $n$ -hexane/EtOAc 4:1 as an eluent,  $R_f = 0.6$ .  $\nu_{\text{max}}$  (KBr) 837, 1103, 1164, 1234, 1508, 1612, 2233, 2943, 3039  $\text{cm}^{-1}$ .  $^1\text{H}$  NMR (250 MHz,  $\text{CDCl}_3$ ):  $\delta$  (ppm) 1.76–1.92 (m, 4H), 3.74 (t,  $J = 5.7$  Hz, 2H), 4.14 (t,  $J = 5.7$  Hz, 2H), 6.86 (d,  $J = 7.8$  Hz, 2H), 7.61 (d,  $J = 7.8$  Hz, 2H).  $^{13}\text{C}$  NMR (62.5 MHz,  $\text{CDCl}_3$ ):  $\delta$  (ppm) 27.2, 31.8, 32.7, 66.2, 103.5, 114.4, 118.1, 133.0, 159.1. Anal. Calcd for  $\text{C}_{11}\text{H}_{12}\text{BrNO}$ : C, 51.99; H, 4.76; N, 5.51%. Found: C, 52.18; H, 4.85; N, 5.37%. MS ( $m/z$ ): 253 ( $\text{M}^+$ ).

#### 4.1.2. General procedure for the silylation of nucleobases

In a 250-mL round-bottom flask, a mixture of the appropriate nucleobase (10 mmol), silica sulfuric acid (0.05 g), and HMDS (100 mL) was heated at reflux until a clear solution was obtained. Then the catalyst was filtered off, and the filtrate was evaporated under vacuum to remove the solvent (HMDS). The resulting crude was pure enough and does not require further purification or characterization.<sup>28</sup>

#### 4.1.3. General procedure for the synthesis of nucleobase-contained nitriles (**5a-n**)

To a double-necked 250-mL round-bottom flask equipped with a

condenser containing an appropriate amount of persilylated nucleobase (10 mmol) and 4-(3-bromopropoxy)benzotrile (4a) (10 mmol, 2.4 g) or 4-(4-bromobutoxy)benzotrile (4b) (10 mmol, 2.5 g) diluted in freshly distilled, anhydrous THF (100 mL), anhydrous TBAF (2.62 g, 10 mmol) in THF solution (20 mL) was gradually added over 20 min. Then, the mixture was heated at reflux temperature (TLC control). After completion of reaction, the solvent was evaporated at reduced pressure, and the residue was dissolved in CHCl<sub>3</sub> (200 mL) and washed with H<sub>2</sub>O (3 × 100 mL). The organic layer was dried (10 g of Na<sub>2</sub>SO<sub>4</sub>) and concentrated to afford the crude products.

**4.1.3.1. 4-(3-(2,4-Dioxo-3,4-dihydropyrimidin-1(2H)-yl)propoxy)benzotrile (5a).** White solid, Purified with column chromatography using *n*-hexane/EtOAc 2:1 as an eluent, *R<sub>f</sub>* = 0.52, Isolated Yield: 80%, M.P. = 148–150 °C. *v*<sub>max</sub> (KBr) 837, 1103, 1164, 1508, 1735, 2233, 2935, 3109, 3210 cm<sup>-1</sup>. <sup>1</sup>H NMR (250 MHz, DMSO-*d*<sub>6</sub>): δ (ppm) 2.19–2.30 (m, 2H), 3.95 (t, *J* = 7.1 Hz, 2H), 4.26 (t, *J* = 7.1 Hz, 2H), 5.39 (d, *J* = 7.3 Hz, 1H), 6.84 (d, *J* = 8.2 Hz, 2H), 7.32 (d, *J* = 7.3 Hz, 1H), 7.56 (d, *J* = 8.2 Hz, 2H), 10.96 (s, 1H). <sup>13</sup>C NMR (62.5 MHz, DMSO-*d*<sub>6</sub>): δ (ppm) 26.6, 40.9, 65.8, 103.6, 106.4, 114.9, 118.7, 133.2, 145.7, 152.0, 160.9, 165.0. Anal. Calcd for C<sub>14</sub>H<sub>13</sub>N<sub>3</sub>O<sub>3</sub>: C, 61.99; H, 4.83; N, 15.49%. Found: C, 62.17; H, 4.67; N, 15.63%.

**4.1.3.2. 4-(3-(3,5-Dioxo-4,5-dihydro-1,2,4-triazin-2(3H)-yl)propoxy)benzotrile (5b).** White solid, Purified with column chromatography using *n*-hexane/EtOAc 2:1 as an eluent, *R<sub>f</sub>* = 0.57, Isolated Yield: 82%, M.P. = 159–161 °C. *v*<sub>max</sub> (KBr) 837, 1018, 1222, 1407, 1585, 1681, 2233, 2904, 3043, 3263 cm<sup>-1</sup>. <sup>1</sup>H NMR (250 MHz, DMSO-*d*<sub>6</sub>): δ (ppm) 2.19–2.29 (m, 2H), 3.86 (t, *J* = 6.2 Hz, 2H), 4.16 (t, *J* = 6.2 Hz, 2H), 6.85 (d, *J* = 8.4 Hz, 2H), 7.34 (s, 1H), 7.58 (d, *J* = 8.4 Hz, 2H), 10.55 (s, 1H). <sup>13</sup>C NMR (62.5 MHz, DMSO-*d*<sub>6</sub>): δ (ppm) 27.5, 41.9, 66.8, 106.3, 114.7, 118.2, 132.3, 136.7, 146.3, 158.1, 162.0. Anal. Calcd for C<sub>13</sub>H<sub>12</sub>N<sub>4</sub>O<sub>3</sub>: C, 57.35; H, 4.44; N, 20.58%. Found: C, 57.51; H, 4.25; N, 20.52%.

**4.1.3.3. 4-(3-(6-Oxo-1,6-dihydropyrimidin-2-yl)thio)propoxy)benzotrile (5c).** White solid, Purified with column chromatography using *n*-hexane/EtOAc 2:1 as an eluent, *R<sub>f</sub>* = 0.63, Isolated Yield: 82%, M.P. = 131–132 °C. *v*<sub>max</sub> (KBr) 837, 1164, 1215, 1508, 1685, 1704, 2233, 2923, 3085, 3274 cm<sup>-1</sup>. <sup>1</sup>H NMR (250 MHz, DMSO-*d*<sub>6</sub>): δ (ppm) 2.23–2.31 (m, 2H), 3.28 (t, *J* = 5.4 Hz, 2H), 3.87 (t, *J* = 5.4 Hz, 2H), 5.79 (d, *J* = 7.5 Hz, 1H), 6.86 (d, *J* = 8.2 Hz, 2H), 7.39 (d, *J* = 7.5 Hz, 1H), 7.59 (d, *J* = 8.2 Hz, 2H), 10.58 (s, 1H). <sup>13</sup>C NMR (62.5 MHz, DMSO-*d*<sub>6</sub>): δ (ppm) 26.1, 28.9, 64.1, 102.1, 109.9, 113.0, 116.7, 131.5, 147.0, 157.0, 157.7, 161.9. Anal. Calcd for C<sub>14</sub>H<sub>13</sub>N<sub>3</sub>O<sub>2</sub>S: C, 58.52; H, 4.56; N, 14.62%. Found: C, 58.70; H, 4.51; N, 14.51%.

**4.1.3.4. 4-(3-(6-Amino-9H-Purine-9-yl)propoxy)benzotrile (5d).** White solid, Purified with column chromatography using *n*-hexane/EtOAc 1:1 as an eluent, *R<sub>f</sub>* = 0.60, Isolated Yield: 82%, M.P. = 155–157 °C. *v*<sub>max</sub> (KBr) 810, 1222, 1419, 1508, 1601, 1670, 2233, 2938, 3120, 3251 cm<sup>-1</sup>. <sup>1</sup>H NMR (250 MHz, DMSO-*d*<sub>6</sub>): δ (ppm) 2.21–2.31 (m, 2H), 3.88 (t, *J* = 6.3 Hz, 2H), 4.14 (t, *J* = 6.3 Hz, 2H), 6.86 (d, *J* = 8.6 Hz, 2H), 7.32 (s, 2H), 7.60 (d, *J* = 8.6 Hz, 2H), 8.12 (s, 1H), 8.29 (s, 1H). <sup>13</sup>C NMR (62.5 MHz, DMSO-*d*<sub>6</sub>): δ (ppm) 27.2, 42.3, 65.2, 102.7, 113.6, 117.3, 117.7, 132.2, 140.5, 147.9, 151.2, 154.3, 158.4. Anal. Calcd for C<sub>15</sub>H<sub>14</sub>N<sub>6</sub>O: C, 61.21; H, 4.79; N, 28.55%. Found: C, 61.45; H, 4.54; N, 28.73%.

**4.1.3.5. 4-(3-(2-Amino-6-oxo-1,6-dihydro-9H-Purine-9-yl)propoxy)benzotrile (5e).** White solid, Purified with column chromatography using *n*-hexane/EtOAc 1:1 as an eluent, *R<sub>f</sub>* = 0.52, Isolated Yield: 70%, M.P. = 148–150 °C. *v*<sub>max</sub> (KBr) 837, 1103, 1284, 1508, 1612, 2233, 2947, 3074, 3286, 3418 cm<sup>-1</sup>. <sup>1</sup>H NMR (250 MHz, DMSO-*d*<sub>6</sub>): δ (ppm) 2.21–2.31 (m, 2H), 3.98 (t, *J* = 6.3 Hz, 2H), 4.24 (t, *J* = 6.3 Hz, 2H), 6.58 (s, 2H), 6.86 (d, *J* = 8.8 Hz, 2H), 7.61 (d, *J* = 8.8 Hz, 2H), 7.98 (s,

1H), 10.59 (s, 1H). <sup>13</sup>C NMR (62.5 MHz, DMSO-*d*<sub>6</sub>): δ (ppm) 27.0, 41.9, 64.9, 102.4, 113.3, 115.3, 117.0, 131.9, 136.8, 149.2, 151.8, 155.3, 158.0. Anal. Calcd for C<sub>15</sub>H<sub>14</sub>N<sub>6</sub>O<sub>2</sub>: C, 58.06; H, 4.55; N, 27.08%. Found: C, 58.21; H, 4.48; N, 27.19%.

**4.1.3.6. 4-(3-(1,3-Dimethyl-2,6-dioxo-1,2,3,6-tetrahydro-7H-Purine-7-yl)propoxy)benzotrile (5f).** White solid, Purified with column chromatography using *n*-hexane/EtOAc 1:1 as an eluent, *R<sub>f</sub>* = 0.62, Isolated Yield: 87%, M.P. = 136–138 °C. *v*<sub>max</sub> (KBr) 837, 1188, 1488, 1558, 1666, 1716, 2233, 2950, 3086 cm<sup>-1</sup>. <sup>1</sup>H NMR (250 MHz, DMSO-*d*<sub>6</sub>): δ (ppm) 2.21–2.30 (m, 2H), 3.20 (s, 3H), 3.39 (s, 3H), 3.97 (t, *J* = 6.9 Hz, 2H), 4.25 (t, *J* = 6.9 Hz, 2H), 6.88 (d, *J* = 8.8 Hz, 2H), 7.61 (d, *J* = 8.8 Hz, 2H), 8.02 (s, 1H). <sup>13</sup>C NMR (62.5 MHz, DMSO-*d*<sub>6</sub>): δ (ppm) 26.4, 26.6, 26.7, 42.3, 64.6, 102.1, 105.0, 113.0, 116.7, 131.6, 139.1, 146.4, 149.4, 152.5, 157.8. Anal. Calcd for C<sub>17</sub>H<sub>17</sub>N<sub>5</sub>O<sub>3</sub>: C, 60.17; H, 5.05; N, 20.64%. Found: C, 60.30; H, 5.25; N, 20.83%.

**4.1.3.7. 4-(3-(3,7-Dimethyl-2,6-dioxo-2,3,6,7-tetrahydro-1H-Purine-1-yl)propoxy)benzotrile (5g).** White solid, Purified with column chromatography using *n*-hexane/EtOAc 1:1 as an eluent, *R<sub>f</sub>* = 0.58, Isolated Yield: 89%, M.P. = 149–152 °C. *v*<sub>max</sub> (KBr) 837, 1164, 1284, 1485, 1693, 2233, 2954, 3028 cm<sup>-1</sup>. <sup>1</sup>H NMR (250 MHz, DMSO-*d*<sub>6</sub>): δ (ppm) 2.22–2.32 (m, 2H), 3.27 (s, 3H), 3.82–3.99 (m, 5H), 4.28 (t, *J* = 7.3 Hz, 2H), 6.87 (d, *J* = 8.6 Hz, 2H), 7.61 (d, *J* = 8.6 Hz, 2H), 7.94 (s, 1H). <sup>13</sup>C NMR (62.5 MHz, DMSO-*d*<sub>6</sub>): δ (ppm) 29.8, 32.6, 34.0, 36.6, 65.7, 103.2, 106.7, 114.1, 117.8, 137.7, 141.2, 147.8, 150.4, 154.2, 158.8. Anal. Calcd for C<sub>17</sub>H<sub>17</sub>N<sub>5</sub>O<sub>3</sub>: C, 60.17; H, 5.05; N, 20.64%. Found: C, 60.36; H, 5.18; N, 20.49%.

**4.1.3.8. 4-(4-(2,4-Dioxo-3,4-dihydropyrimidin-1(2H)-yl)butoxy)benzotrile (5h).** White solid, Purified with column chromatography using *n*-hexane/EtOAc 2:1 as an eluent, *R<sub>f</sub>* = 0.52, Isolated Yield: 80%, M.P. = 141–142 °C. *v*<sub>max</sub> (KBr) 837, 1164, 1234, 1508, 1735, 2233, 2935, 3109, 3207 cm<sup>-1</sup>. <sup>1</sup>H NMR (250 MHz, DMSO-*d*<sub>6</sub>): δ (ppm) 1.85–2.02 (m, 4H), 3.93 (t, *J* = 5.8 Hz, 2H), 4.04 (t, *J* = 5.8 Hz, 2H), 5.38 (d, *J* = 7.1 Hz, 1H), 6.96 (d, *J* = 7.8 Hz, 2H), 7.33 (d, *J* = 7.1 Hz, 1H), 7.70 (d, *J* = 7.8 Hz, 2H), 10.6 (s, 1H). <sup>13</sup>C NMR (62.5 MHz, DMSO-*d*<sub>6</sub>): δ (ppm) 23.5, 23.7, 43.7, 64.9, 99.2, 101.2, 112.1, 115.8, 130.7, 144.0, 149.6, 156.8, 162.7. Anal. Calcd for C<sub>15</sub>H<sub>15</sub>N<sub>3</sub>O<sub>3</sub>: C, 63.15; H, 5.30; N, 14.73%. Found: C, 63.01; H, 5.44; N, 14.52%.

**4.1.3.9. 4-(4-(3,5-Dioxo-4,5-dihydro-1,2,4-triazin-2(3H)-yl)butoxy)benzotrile (5i).** White solid, Purified with column chromatography using *n*-hexane/EtOAc 2:1 as an eluent, *R<sub>f</sub>* = 0.55, Isolated Yield: 82%, M.P. = 156–157 °C. *v*<sub>max</sub> (KBr) 837, 1164, 1284, 1407, 1585, 1685, 2233, 2904, 3047, 3251 cm<sup>-1</sup>. <sup>1</sup>H NMR (250 MHz, DMSO-*d*<sub>6</sub>): δ (ppm) 1.76–1.95 (m, 4H), 3.94 (t, *J* = 6.3 Hz, 2H), 4.15 (t, *J* = 6.3 Hz, 2H), 6.87 (d, *J* = 8.7 Hz, 2H), 7.36 (s, 1H), 7.61 (d, *J* = 8.7 Hz, 2H), 10.5 (s, 1H). <sup>13</sup>C NMR (62.5 MHz, DMSO-*d*<sub>6</sub>): δ (ppm) 25.9, 26.1, 44.5, 67.1, 103.4, 114.3, 118.0, 132.9, 135.5, 147.3, 156.6, 159.1. Anal. Calcd for C<sub>14</sub>H<sub>14</sub>N<sub>4</sub>O<sub>3</sub>: C, 58.74; H, 4.93; N, 19.57%. Found: C, 58.88; H, 5.09; N, 19.80%.

**4.1.3.10. 4-(4-(6-Oxo-1,6-dihydropyrimidin-2-yl)thio)butoxy)benzotrile (5j).** White solid, Purified with column chromatography using *n*-hexane/EtOAc 2:1 as an eluent, *R<sub>f</sub>* = 0.60, Isolated Yield: 80%, M.P. = 136–139 °C. *v*<sub>max</sub> (KBr) 837, 1164, 1508, 1685, 2233, 2931, 3043, 3271 cm<sup>-1</sup>. <sup>1</sup>H NMR (250 MHz, DMSO-*d*<sub>6</sub>): δ (ppm) 1.58–1.68 (m, 4H), 3.24 (t, *J* = 6.0 Hz, 2H), 4.15 (t, *J* = 6.0 Hz, 2H), 5.79 (d, *J* = 7.6 Hz, 1H), 6.87 (d, *J* = 8.6 Hz, 2H), 7.36 (d, *J* = 7.6 Hz, 1H), 7.61 (d, *J* = 8.6 Hz, 2H), 10.58 (s, 1H). <sup>13</sup>C NMR (62.5 MHz, DMSO-*d*<sub>6</sub>): δ (ppm) 24.2, 25.0, 29.1, 67.4, 100.1, 110.6, 113.0, 116.7, 131.5, 141.5, 157.0, 157.7, 159.7. Anal. Calcd for C<sub>15</sub>H<sub>15</sub>N<sub>3</sub>O<sub>2</sub>S: C, 59.78; H, 5.02; N, 13.94%. Found: C, 59.92; H, 4.83; N, 14.14%.

**4.1.3.11. 4-(4-(6-Amino-9H-Purine-9-yl)butoxy)benzotrile (5k).** White solid, Purified with column chromatography using *n*-hexane/EtOAc 1:1 as

an eluent,  $R_f = 0.58$ ), Isolated Yield: 84%, M.P. = 149–152 °C.  $\nu_{\max}$  (KBr) 840, 1307, 1508, 1604, 1670, 2233, 2958, 3120, 3294  $\text{cm}^{-1}$ .  $^1\text{H}$  NMR (250 MHz, DMSO- $d_6$ ):  $\delta$  (ppm) 1.76–1.95 (m, 4H), 3.94 (t,  $J = 6.3$  Hz, 2H), 4.15 (t,  $J = 6.3$  Hz, 2H), 6.86 (d,  $J = 8.4$  Hz, 2H), 7.39 (s, 2H), 7.61 (d,  $J = 8.4$  Hz, 2H), 8.14 (s, 1H), 8.29 (s, 1H).  $^{13}\text{C}$  NMR (62.5 MHz, DMSO- $d_6$ ):  $\delta$  (ppm) 25.7, 25.9, 43.0, 67.1, 103.4, 114.3, 118.0, 118.4, 132.9, 139.6, 148.6, 151.9, 155.0, 159.1. Anal. Calcd for  $\text{C}_{16}\text{H}_{16}\text{N}_6\text{O}$ : C, 62.32; H, 5.23; N, 27.26%. Found: C, 61.99; H, 5.17; N, 27.51%.

#### 4.1.3.12. 4-(4-(2-Amino-6-oxo-1,6-dihydro-9H-Purine-9-yl)butoxy)benzotrile (5 l)

White solid, Purified with column chromatography using *n*-hexane/EtOAc 1:1 as an eluent,  $R_f = 0.50$ , Isolated Yield: 69%, M.P. = 148–149 °C.  $\nu_{\max}$  (KBr) 837, 1103, 1284, 1508, 1612, 2233, 2947, 3078, 3290  $\text{cm}^{-1}$ .  $^1\text{H}$  NMR (250 MHz, DMSO- $d_6$ ):  $\delta$  (ppm) 1.77–1.93 (m, 4H), 3.94 (t,  $J = 6.1$  Hz, 2H), 4.14 (t,  $J = 6.1$  Hz, 2H), 6.58 (s, 2H), 6.87 (d,  $J = 8.8$  Hz, 2H), 7.60 (d,  $J = 8.8$  Hz, 2H), 7.92 (s, 1H), 10.58 (s, 1H).  $^{13}\text{C}$  NMR (62.5 MHz, DMSO- $d_6$ ):  $\delta$  (ppm) 25.2, 25.5, 41.2, 66.7, 103.0, 113.8, 115.8, 117.6, 132.4, 136.7, 150.3, 152.3, 155.8, 158.6. Anal. Calcd for  $\text{C}_{16}\text{H}_{16}\text{N}_6\text{O}_2$ : C, 59.25; H, 4.97; N, 25.91%. Found: C, 59.42; H, 5.26; N, 25.98%.

4.1.3.13. 4-(4-(1,3-Dimethyl-2,6-dioxo-1,2,3,6-tetrahydro-7H-Purine-7-yl)butoxy)benzotrile (5 m). White solid, Purified with column chromatography using *n*-hexane/EtOAc 1:1 as an eluent,  $R_f = 0.67$ , Isolated Yield: 89%, M.P. = 131–133 °C.  $\nu_{\max}$  (KBr) 837, 1188, 1284, 1666, 1716, 2233, 2970, 3089  $\text{cm}^{-1}$ .  $^1\text{H}$  NMR (250 MHz, DMSO- $d_6$ ):  $\delta$  (ppm) 1.77–1.91 (m, 4H), 3.19 (s, 3H), 3.40 (s, 3H), 3.93 (t,  $J = 6.2$  Hz, 2H), 4.03 (t,  $J = 6.2$  Hz, 2H), 6.86 (d,  $J = 8.6$  Hz, 2H), 7.59 (d,  $J = 8.6$  Hz, 2H), 7.99 (s, 1H).  $^{13}\text{C}$  NMR (62.5 MHz, DMSO- $d_6$ ):  $\delta$  (ppm) 24.4, 24.6, 26.4, 26.6, 44.0, 65.8, 102.1, 105.0, 113.0, 116.7, 131.6, 139.1, 146.4, 149.4, 152.5, 157.8. Anal. Calcd for  $\text{C}_{18}\text{H}_{19}\text{N}_5\text{O}_3$ : C, 61.18; H, 5.42; N, 19.82%. Found: C, 60.62; H, 5.81; N, 20.13%.

4.1.3.14. 4-(4-(3,7-Dimethyl-2,6-dioxo-2,3,6,7-tetrahydro-1H-Purine-1-yl)butoxy)benzotrile (5n). White solid, Purified with column chromatography using *n*-hexane/EtOAc 1:1 as an eluent,  $R_f = 0.63$ , Isolated Yield: 89%, M.P. = 145–147 °C.  $\nu_{\max}$  (KBr) 837, 1222, 1685, 2233, 2823, 3024  $\text{cm}^{-1}$ .  $^1\text{H}$  NMR (250 MHz, DMSO- $d_6$ ):  $\delta$  (ppm) 1.75–1.96 (m, 4H), 3.31 (s, 3H), 3.81 (s, 3H), 3.95 (t,  $J = 6.2$  Hz, 2H), 4.14 (t,  $J = 6.2$  Hz, 2H), 6.87 (d,  $J = 8.8$  Hz, 2H), 7.61 (d,  $J = 8.8$  Hz, 2H), 7.95 (s, 1H).  $^{13}\text{C}$  NMR (62.5 MHz, DMSO- $d_6$ ):  $\delta$  (ppm) 25.73, 25.76, 32.6, 34.0, 40.3, 66.9, 103.2, 106.7, 114.1, 117.8, 132.7, 141.2, 147.8, 150.5, 154.3, 158.8. Anal. Calcd for  $\text{C}_{18}\text{H}_{19}\text{N}_5\text{O}_3$ : C, 61.18; H, 5.42; N, 19.82%. Found: C, 60.86; H, 5.65; N, 20.09%.

#### 4.1.4. General procedure for the synthesis of nucleobase-contained hybrids of tetrazoles (6a-n)

To a 250 mL round-bottomed flask was added the nucleobase-contained nitrile (5a-n) (20 mmol), sodium azide (30 mmol, 1.95 g), zinc bromide (4.50 g, 20 mmol), and 40 mL of water. The reaction mixture was refluxed for 24 h. (Vigorous stirring is essential). HCl (3 N, 30 mL) and ethyl acetate (100 mL) were added, and vigorous stirring was continued until no solid was present and the aqueous layer had a pH of 1. If necessary, additional ethyl acetate was added. The organic layer was isolated and the aqueous layer extracted with 2 × 100 mL of ethyl acetate. The combined organic layers were evaporated, 200 mL of 0.25 N NaOH was added, and the mixture was stirred for 30 min, until the original precipitate was dissolved and a suspension of zinc hydroxide was formed. The suspension was filtered, and the solid washed with 20 mL of 1 N NaOH. To the filtrate was added 40 mL of 3 N HCl with vigorous stirring causing the tetrazole to precipitate. The tetrazole was filtered and washed with 2 × 20 mL of HCl (3 N) and dried in a drying oven to furnish the nucleobase-contained hybrids of tetrazole (6a-n) as white solids.

4.1.4.1. 1-(3-(4-(1H-Tetrazol-5-yl)phenoxy)propyl)pyrimidine-2,4 (1H, 3H)-dione (6a). White solid, M.P. = 189–191 °C.  $\nu_{\max}$  (KBr) 840,

1080, 1234, 1419, 1515, 1620, 1712, 2630, 2738, 2823, 2845, 2927, 3030, 3101, 3427  $\text{cm}^{-1}$ .  $^1\text{H}$  NMR (250 MHz, DMSO- $d_6$ ):  $\delta$  (ppm) 2.20–2.30 (m, 2H), 4.03 (t,  $J = 6.5$  Hz, 2H), 4.13 (t,  $J = 6.5$  Hz, 2H), 5.18 (d,  $J = 6.4$  Hz, 1H), 6.85 (d,  $J = 7.6$  Hz, 2H), 7.14 (d,  $J = 6.4$  Hz, 1H), 7.76 (d,  $J = 7.6$  Hz, 2H), 10.50 (s, 1H).  $^{13}\text{C}$  NMR (62.5 MHz, DMSO- $d_6$ ):  $\delta$  (ppm) 28.2, 44.2, 66.1, 101.6, 113.9, 122.0, 127.0, 146.4, 152.0, 154.2, 159.9, 165.1. Anal. Calcd for  $\text{C}_{14}\text{H}_{14}\text{N}_6\text{O}_3$ : C, 53.50; H, 4.49; N, 26.74%. Found: C, 53.61; H, 4.33; N, 26.86%. MS ( $m/z$ ): 314 ( $\text{M}^+$ ).

4.1.4.2. 2-(3-(4-(1H-Tetrazol-5-yl)phenoxy)propyl)-1,2,4-triazine-3,5 (2H, 4H)-dione (6b). White solid, M.P. = 212–213 °C.  $\nu_{\max}$  (KBr) 840, 1018, 1265, 1404, 1450, 1651, 2700, 2800, 2854, 2916, 3039, 3155, 3460  $\text{cm}^{-1}$ .  $^1\text{H}$  NMR (250 MHz, DMSO- $d_6$ ):  $\delta$  (ppm) 2.10–2.21 (m, 2H), 3.99 (t,  $J = 6.7$  Hz, 2H), 4.28 (t,  $J = 6.7$  Hz, 2H), 6.79 (d,  $J = 7.5$  Hz, 2H), 7.28 (s, 1H), 7.71 (d,  $J = 7.5$  Hz, 2H), 10.45 (s, 1H).  $^{13}\text{C}$  NMR (62.5 MHz, DMSO- $d_6$ ):  $\delta$  (ppm) 28.3, 43.0, 66.3, 114.2, 122.2, 127.2, 135.9, 147.7, 154.5, 157.0, 160.2. Anal. Calcd for  $\text{C}_{13}\text{H}_{13}\text{N}_7\text{O}_3$ : C, 49.52; H, 4.16; N, 31.10%. Found: C, 49.68; H, 4.18; N, 30.98%.

4.1.4.3. 2-((3-(4-(1H-Tetrazol-5-yl)phenoxy)propyl)thio)pyrimidin-4 (3H)-one (6c). White solid, M.P. = 170–172 °C.  $\nu_{\max}$  (KBr) 833, 1172, 1450, 1519, 1620, 2710, 2835, 2875, 2923, 3047, 3150, 3425  $\text{cm}^{-1}$ .  $^1\text{H}$  NMR (250 MHz, DMSO- $d_6$ ):  $\delta$  (ppm) 1.73–1.83 (m, 2H), 3.25 (t,  $J = 6.5$  Hz, 2H), 4.20 (t,  $J = 6.5$  Hz, 2H), 6.10 (d,  $J = 6.5$  Hz, 1H), 6.66 (d,  $J = 7.5$  Hz, 2H), 7.66 (d,  $J = 7.4$  Hz, 2H), 7.84 (d,  $J = 6.5$  Hz, 1H), 10.16 (s, 1H).  $^{13}\text{C}$  NMR (62.5 MHz, DMSO- $d_6$ ):  $\delta$  (ppm) 25.5, 29.8, 67.5, 102.5, 111.7, 115.2, 124.8, 146.3, 149.3, 156.4, 157.8, 165.8. Anal. Calcd for  $\text{C}_{14}\text{H}_{14}\text{N}_6\text{O}_2\text{S}$ : C, 50.90; H, 4.27; N, 25.44%. Found: C, 50.99; H, 4.41; N, 25.55%. MS ( $m/z$ ): 330 ( $\text{M}^+$ ).

4.1.4.4. 9-(3-(4-(1H-Tetrazol-5-yl)phenoxy)propyl)-9H-Purine-6-amine (6d). White solid, M.P. = 229–231 °C.  $\nu_{\max}$  (KBr) 840, 1249, 1419, 1604, 1666, 2630, 2692, 2720, 2831, 2950, 3041, 3103, 3294, 3407  $\text{cm}^{-1}$ .  $^1\text{H}$  NMR (250 MHz, DMSO- $d_6$ ):  $\delta$  (ppm) 2.18–2.28 (m, 2H), 4.00 (t,  $J = 6.0$  Hz, 2H), 4.26 (t,  $J = 6.0$  Hz, 2H), 6.83 (d,  $J = 7.1$  Hz, 2H), 7.30 (s, 2H), 7.82 (d,  $J = 7.1$  Hz, 2H), 8.13 (s, 1H), 8.25 (s, 1H).  $^{13}\text{C}$  NMR (62.5 MHz, DMSO- $d_6$ ):  $\delta$  (ppm) 27.5, 42.6, 65.6, 113.4, 118.1, 121.5, 126.5, 140.9, 148.2, 151.6, 153.8, 154.6, 156.5. Anal. Calcd for  $\text{C}_{15}\text{H}_{15}\text{N}_9\text{O}$ : C, 53.41; H, 4.48; N, 37.37%. Found: C, 53.59; H, 4.39; N, 37.52%.

4.1.4.5. 9-(3-(4-(1H-Tetrazol-5-yl)phenoxy)propyl)-2-amino-1,9-dihydro-6H-Purine-6-one (6e). White solid, M.P. = 221–223 °C.  $\nu_{\max}$  (KBr) 840, 1080, 1249, 1411, 1512, 1612, 2630, 2707, 2854, 2931, 3024, 3130, 3305, 3425  $\text{cm}^{-1}$ .  $^1\text{H}$  NMR (250 MHz, DMSO- $d_6$ ):  $\delta$  (ppm) 2.25–2.35 (m, 2H), 4.10 (t,  $J = 6.2$  Hz, 2H), 4.28 (t,  $J = 6.2$  Hz, 2H), 6.66 (s, 2H), 6.79 (d,  $J = 7.4$  Hz, 2H), 7.70 (d,  $J = 7.4$  Hz, 2H), 8.29 (s, 1H), 10.61 (s, 1H).  $^{13}\text{C}$  NMR (62.5 MHz, DMSO- $d_6$ ):  $\delta$  (ppm) 28.0, 42.9, 65.9, 113.7, 116.3, 121.8, 126.8, 137.8, 150.2, 152.8, 154.0, 156.3, 159.7. Anal. Calcd for  $\text{C}_{15}\text{H}_{15}\text{N}_9\text{O}_2$ : C, 50.99; H, 4.28; N, 35.68%. Found: C, 50.74; H, 4.12; N, 35.82%.

4.1.4.6. 7-(3-(4-(1H-Tetrazol-5-yl)phenoxy)propyl)-1,3-dimethyl-3,7-dihydro-1H-Purine-2,6-dione (6f). White solid, M.P. = 238–241 °C.  $\nu_{\max}$  (KBr) 840, 1188, 1442, 1566, 1666, 2607, 2715, 2854, 2923, 3062, 3124, 3409  $\text{cm}^{-1}$ .  $^1\text{H}$  NMR (250 MHz, DMSO- $d_6$ ):  $\delta$  (ppm) 2.18–2.28 (m, 2H), 3.13 (s, 3H), 3.31 (s, 3H), 4.01 (t,  $J = 6.2$  Hz, 2H), 4.31 (t,  $J = 6.2$  Hz, 2H), 6.84 (d,  $J = 7.7$  Hz, 2H), 7.79 (d,  $J = 7.7$  Hz, 2H), 8.00 (s, 1H).  $^{13}\text{C}$  NMR (62.5 MHz, DMSO- $d_6$ ):  $\delta$  (ppm) 27.8, 28.0, 28.1, 23.7, 66.0, 106.4, 113.9, 121.9, 126.9, 140.5, 147.8, 150.8, 153.9, 154.2, 159.9. Anal. Calcd for  $\text{C}_{17}\text{H}_{18}\text{N}_8\text{O}_3$ : C, 53.40; H, 4.74; N, 29.30%. Found: C, 53.69; H, 4.71; N, 29.29%.

4.1.4.7. 1-(3-(4-(1H-Tetrazol-5-yl)phenoxy)propyl)-3,7-dimethyl-3,7-dihydro-1H-Purine-2,6-dione (6 g). White solid, M.P. = 219–222 °C.

$\nu_{\max}$  (KBr) 840, 1226, 1450, 1542, 1691, 2610, 2750, 2823, 2890, 2955, 3024, 3451  $\text{cm}^{-1}$ .  $^1\text{H}$  NMR (250 MHz, DMSO- $d_6$ ):  $\delta$  (ppm) 2.21–2.31 (m, 2H), 3.35 (s, 3H), 3.83 (s, 3H), 4.05 (t,  $J = 6.4$  Hz, 2H), 4.32 (t,  $J = 6.4$  Hz, 2H), 6.79 (d,  $J = 7.3$  Hz, 2H), 7.73 (d,  $J = 7.3$  Hz, 2H), 8.00 (s, 1H).  $^{13}\text{C}$  NMR (62.5 MHz, DMSO- $d_6$ ):  $\delta$  (ppm) 29.4, 32.2, 33.6, 36.3, 65.3, 106.3, 113.2, 121.2, 126.3, 140.6, 147.4, 150.0, 153.5, 153.8, 159.2. Anal. Calcd for  $\text{C}_{17}\text{H}_{18}\text{N}_8\text{O}_3$ : C, 53.40; H, 4.74; N, 29.30%. Found: C, 53.58; H, 4.34; N, 29.01%.

4.1.4.8. 1-(4-(4-(1H-Tetrazol-5-yl)phenoxy)butyl)pyrimidine-2,4(1H,3H)-dione (6h). White solid, M.P. = 208–210 °C.  $\nu_{\max}$  (KBr) 840, 1080, 1234, 1419, 1651, 1735, 2491, 2630, 2731, 2823, 2854, 29313040, 3101, 3425  $\text{cm}^{-1}$ .  $^1\text{H}$  NMR (250 MHz, DMSO- $d_6$ ):  $\delta$  (ppm) 1.94–2.12 (m, 4H), 4.01 (t,  $J = 6.2$  Hz, 2H), 4.26 (t,  $J = 6.2$  Hz, 2H), 5.19 (d,  $J = 6.5$  Hz, 1H), 6.91 (d,  $J = 7.8$  Hz, 2H), 7.14 (d,  $J = 6.5$  Hz, 1H), 7.61 (d,  $J = 7.8$  Hz, 2H), 10.56 (s, 1H).  $^{13}\text{C}$  NMR (62.5 MHz, DMSO- $d_6$ ):  $\delta$  (ppm) 26.1, 26.2, 46.7, 67.8, 101.9, 115.0, 121.7, 127.5, 148.6, 151.9, 154.3, 161.7, 165.5. Anal. Calcd for  $\text{C}_{15}\text{H}_{16}\text{N}_6\text{O}_3$ : C, 54.87; H, 4.91; N, 25.60%. Found: C, 55.01; H, 4.83; N, 25.69%.

4.1.4.9. 2-(4-(4-(1H-Tetrazol-5-yl)phenoxy)butyl)-1,2,4-triazine-3,5(2H,4H)-dione (6i). White solid, M.P. = 212–214 °C.  $\nu_{\max}$  (KBr) 840, 1080, 1411, 1612, 1681, 1712, 2630, 2707, 2800, 2931, 3030, 3153, 3423  $\text{cm}^{-1}$ .  $^1\text{H}$  NMR (250 MHz, DMSO- $d_6$ ):  $\delta$  (ppm) 1.79–2.00 (m, 4H), 4.03 (t,  $J = 6.3$  Hz, 2H), 4.21 (t,  $J = 6.3$  Hz, 2H), 6.92 (d,  $J = 7.4$  Hz, 2H), 7.36 (s, 1H), 7.85 (d,  $J = 7.4$  Hz, 2H), 10.16 (s, 1H).  $^{13}\text{C}$  NMR (62.5 MHz, DMSO- $d_6$ ):  $\delta$  (ppm) 26.12, 16.19, 46.4, 65.3, 113.9, 121.9, 127.8, 135.6, 148.6, 153.0, 158.5, 161.2. Anal. Calcd for  $\text{C}_{14}\text{H}_{15}\text{N}_7\text{O}_3$ : C, 51.06; H, 4.59; N, 29.77%. Found: C, 50.78; H, 4.7; N, 30.01%.

4.1.4.10. 2-(4-(4-(1H-Tetrazol-5-yl)phenoxy)butyl)thio)pyrimidin-4(3H)-one (6j). White solid, M.P. = 185–188 °C.  $\nu_{\max}$  (KBr) 840, 1172, 1211, 1280, 1512, 1612, 1681, 1710, 2630, 2746, 2854, 2931, 3047, 3440  $\text{cm}^{-1}$ .  $^1\text{H}$  NMR (250 MHz, DMSO- $d_6$ ):  $\delta$  (ppm) 1.42–1.62 (m, 4H), 3.26 (t,  $J = 6.5$  Hz, 2H), 4.19 (t,  $J = 6.5$  Hz, 2H), 6.08 (d,  $J = 6.4$  Hz, 1H), 6.89 (d,  $J = 7.4$  Hz, 2H), 7.60 (d,  $J = 7.4$  Hz, 1H), 7.60 (d,  $J = 7.4$  Hz, 1H), 7.84 (d,  $J = 6.4$  Hz, 1H), 10.15 (s, 1H).  $^{13}\text{C}$  NMR (62.5 MHz, DMSO- $d_6$ ):  $\delta$  (ppm) 24.2, 24.7, 31.7, 67.4, 104.1, 112.4, 116.3, 125.5, 147.0, 152.7, 157.0, 158.8, 165.0. Anal. Calcd for  $\text{C}_{15}\text{H}_{16}\text{N}_6\text{O}_2\text{S}$ : C, 52.31; H, 4.68; N, 24.40%. Found: C, 52.50; H, 4.72; N, 24.51%.

4.1.4.11. 9-(4-(4-(1H-Tetrazol-5-yl)phenoxy)butyl)-9H-Purine-6-amine (6k). White solid, M.P. = 216–218 °C.  $\nu_{\max}$  (KBr) 840, 1180, 1419, 1512, 1604, 1674, 2630, 2707, 2850, 2939, 3101, 3294, 3370  $\text{cm}^{-1}$ .  $^1\text{H}$  NMR (250 MHz, DMSO- $d_6$ ):  $\delta$  (ppm) 1.84–2.05 (m, 4H), 4.03 (t,  $J = 6.3$  Hz, 2H), 4.19 (t,  $J = 6.3$  Hz, 2H), 6.86 (d,  $J = 7.4$  Hz, 2H), 7.36 (s, 2H), 7.80 (d,  $J = 7.4$  Hz, 2H), 8.14 (s, 1H), 8.29 (s, 1H).  $^{13}\text{C}$  NMR (62.5 MHz, DMSO- $d_6$ ):  $\delta$  (ppm) 26.1, 26.4, 23.4, 67.6, 114.2, 118.9, 122.2, 127.3, 140.1, 149.0, 152.3, 154.5, 155.4, 160.6. Anal. Calcd for  $\text{C}_{16}\text{H}_{17}\text{N}_9\text{O}$ : C, 54.69; H, 4.88; N, 35.88%. Found: C, 54.78; H, 4.64; N, 35.60%. MS ( $m/z$ ): 367 ( $\text{M}^+$ ).

4.1.4.12. 9-(4-(4-(1H-Tetrazol-5-yl)phenoxy)butyl)-2-amino-1,9-dihydro-6H-Purine-6-one (6l). White solid, M.P. = 225–227 °C.  $\nu_{\max}$  (KBr) 840, 1080, 1249, 1473, 1504, 1612, 2630, 2750, 2854, 2931, 3062, 3301  $\text{cm}^{-1}$ .  $^1\text{H}$  NMR (250 MHz, DMSO- $d_6$ ):  $\delta$  (ppm) 1.86–2.05 (m, 4H), 4.03 (t,  $J = 6.3$  Hz, 2H), 4.19 (t,  $J = 6.3$  Hz, 2H), 6.59 (s, 2H), 6.86 (d,  $J = 7.3$  Hz, 2H), 7.61 (d,  $J = 7.3$  Hz, 2H), 7.93 (s, 1H), 10.51 (s, 1H).  $^{13}\text{C}$  NMR (62.5 MHz, DMSO- $d_6$ ):  $\delta$  (ppm) 25.4, 25.6, 41.4, 66.8, 113.4, 116.0, 121.5, 126.5, 136.9, 150.5, 152.5, 153.8, 156.0, 159.9. Anal. Calcd for  $\text{C}_{16}\text{H}_{17}\text{N}_9\text{O}_2$ : C, 52.31; H, 4.66; N, 34.31%. Found: C, 52.67; H, 4.50; N, 34.48%.

4.1.4.13. 7-(4-(4-(1H-Tetrazol-5-yl)phenoxy)butyl)-1,3-dimethyl-3,7-dihydro-1H-Purine-2,6-dione (6m). White solid, M.P. = 200–203 °C.  $\nu_{\max}$  (KBr) 840, 1280, 1504, 1558, 1651, 1705, 2638, 2715, 2792,

2850, 2931, 3070, 3310  $\text{cm}^{-1}$ .  $^1\text{H}$  NMR (250 MHz, DMSO- $d_6$ ):  $\delta$  (ppm) 1.91–2.12 (m, 4H), 3.19 (s, 3H), 3.40 (s, 3H), 3.89 (t,  $J = 5.9$  Hz, 2H), 4.00 (t,  $J = 5.9$  Hz, 2H), 6.91 (d,  $J = 7.4$  Hz, 2H), 7.81 (d,  $J = 7.4$  Hz, 2H), 7.99 (s, 1H).  $^{13}\text{C}$  NMR (62.5 MHz, DMSO- $d_6$ ):  $\delta$  (ppm) 25.3, 25.6, 27.6, 27.9, 45.9, 67.3, 106.9, 113.7, 121.4, 127.4, 140.9, 147.6, 151.2, 153.7, 153.9, 161.2. Anal. Calcd for  $\text{C}_{18}\text{H}_{20}\text{N}_8\text{O}_3$ : C, 54.54; H, 5.09; N, 28.27%. Found: C, 54.28; H, 5.00; N, 28.44%.

4.1.4.14. 1-(4-(4-(1H-Tetrazol-5-yl)phenoxy)butyl)-3,7-dimethyl-3,7-dihydro-1H-Purine-2,6-dione (6n). White solid, M.P. = 220–223 °C.  $\nu_{\max}$  (KBr) 840, 1226, 1458, 1612, 1697, 2630, 1754, 1823, 2931, 3024, 3309  $\text{cm}^{-1}$ .  $^1\text{H}$  NMR (250 MHz, DMSO- $d_6$ ):  $\delta$  (ppm) 1.98–2.09 (m, 4H), 3.34 (s, 3H), 3.85 (s, 3H), 3.98 (t,  $J = 6.0$  Hz, 2H), 4.25 (t,  $J = 6.0$  Hz, 2H), 6.90 (d,  $J = 7.4$  Hz, 2H), 7.64 (d,  $J = 7.4$  Hz, 2H), 7.98 (s, 1H).  $^{13}\text{C}$  NMR (62.5 MHz, DMSO- $d_6$ ):  $\delta$  (ppm) 26.0, 26.1, 32.9, 34.3, 40.7, 67.2, 107.0, 113.9, 121.9, 126.9, 141.5, 148.1, 150.8, 154.2, 154.6, 160.3. Anal. Calcd for  $\text{C}_{18}\text{H}_{20}\text{N}_8\text{O}_3$ : C, 54.54; H, 5.09; N, 28.27%. Found: C, 54.78; H, 5.23; N, 28.40%. MS ( $m/z$ ): 396 ( $\text{M}^+$ ).

## 4.2. Biology

### 4.2.1. Phosphodiesterase 3A activity assay

The PDE 3A activity assay was done using a reported procedure.<sup>30</sup> An IMAP TR-FRET phosphodiesterase assay kit was used to determine PDE3 activity. This assay was based on hydrolysis of a diester bond in fluorescein-labelled cAMP by PDE3. Both AMP-fluorescein and Phospho-Tb-Donor then bind to the immobilized metal (MIII) coordination complexes on the nanoparticles (IMAP). This type of binding brings the fluorophore and the nucleotide mono phosphate in close proximity to the Tb-Donor so that Fluorescence Resonance Energy Transfer (FRET) is generated upon excitation of FAM. Due to the long lifetime of the Tb-Donor, fluorescence intensities can be measured in a time-resolved mode, which further reduces the background fluorescence created by the cell components. Briefly, 10  $\mu\text{L}$  of diluted phosphodiesterase 3A human (E8784 Sigma) enzyme and 10  $\mu\text{L}$  of the substrate solution, prepared by adding 3  $\mu\text{L}$  of the 100  $\mu\text{M}$  cAMP substrate solution per 1500  $\mu\text{L}$  of complete reaction buffer, were mixed in each of the microplate wells. For the buffer-only control and the Tb-only control, 10  $\mu\text{L}$  of enzyme dilution buffer and 10  $\mu\text{L}$  complete reaction buffer were added to the assigned wells. Then, the plate was incubated at room temperature for 60 min. Then 60  $\mu\text{L}$  IMAP binding solution, containing 70% binding buffer A, 30% binding buffer B and binding reagent 1:800, and Tb-Donor 1:400 (all of these reagents were provided in the kit) were added to all the wells, including the “Tb-only control” wells. Then, 60  $\mu\text{L}$  of binding solution without Tb-Donor was added to the “buffer-only control” wells. The plate was then incubated at room temperature for 3 h. Finally the fluorescence intensities were determined according to the appropriate wavelength for Tb intensities and TR-FRET using Synergy H4 Hybrid Multi-Mode Microplate Reader (BioTek, Model: H4MLFPTAD). The corrected FRET ratio, which has a direct correlation with

PDE activity, was calculated using Equation 1, as follows:

$$\text{Corrected FRET ratio} = \left[ \frac{\text{FRET}_{\text{sample}} - (P * \text{Sample}_{490})}{\text{Sample}_{490}} \right] * 10,000$$

where  $\text{FRET}_{\text{sample}}$  = RFU at 520 nm in one assay well, minus average RFU at 520 nm in the buffer-only control,  $\text{Sample}_{490}$  = RFU at 490 nm in one assay well, minus average RFU at 490 nm in the buffer-only control,  $P$  (a correction coefficient for Tb-Donor contribution to the FRET signal =  $\text{Tb}_{520}/\text{Tb}_{490}$ ),  $\text{Tb}_{520}$  = average RFU at 520 nm in the Terbium-only control, minus average RFU at 520 nm in the buffer-only control and  $\text{Tb}_{490}$  = RFU at 490 nm in the Terbium-only control minus RFU at 490 nm in the buffer-only control.

### 4.2.2. The cytotoxicity study

The cytotoxicity behaviors of synthesized compounds was studied on HeLa and MCF-7 cell lines were obtained from the National Cell Bank of

Iran, Pasteur Institute of Iran. The cells were cultured in DMEM medium supplemented with 10% (v/v) heat-inactivated foetal bovine serum, 100 U/mL penicillin and 100 mg/mL streptomycin, at 37 °C in a humidified atmosphere (95%) containing 5% CO<sub>2</sub>. The MTT [3-(4,5-Dimethylthiazol-2-yl)-2,5-diphenyltetrazolium bromide] assay on HeLa as well as MCF-7 cell line was performed using the reported methods by Hadizadeh *et al.*<sup>31</sup> and Takkol-Afshari *et al.*<sup>32</sup> respectively. So briefly, in a 96-well plate, 5000 HeLa cells/wells or 10,000 MCF-7 cells/wells were seeded and cultured overnight. After this time, different concentrations of synthesized compounds (0.0, 6.25, 12.5, 25.0, 50.0 100.0 and 200.0 μM) were added to each well and incubated for 24 h, the cells were treated with MTT solution (0.5 mg/mL) for 4 h at 37 °C. After this, the medium was removed and obtained formazan crystals were dissolved in dimethylsulfoxide (150 μL) and the absorbance of obtained solutions was measured at 545 nm and 630 nm as a reference (BioTek Synergy H4 Multi-Mode microplate reader). All IC<sub>50</sub>s were calculated with Prism 5.0 software (<http://www.graphpad.com/scientific-software/prism/>).

#### 4.2.3. Docking study

Molecular docking studies were performed to gain a better understanding of the mechanism and potency of the synthesized compounds and to determine their binding site and binding modes. Docking studies were done by AutoDock 4.2 (<http://autodock.scripps.edu>) and AutoDock Tools (ADT) version 1.5.6 programs (<http://mglttools.scripps.edu/>). In silico docking studies were carried out with a homology model of PDE3A target (PDB code: 1LRC.pdb) that it was downloaded from the protein data bank (<http://www.rcsb.org>) opened in AutoDock tools and prepared for docking after adding polar hydrogens. 3D structures of ligands were drawn and minimized under Molecular Mechanics MM<sup>+</sup> and then Semi-empirical AM1 methods using HyperChem 8 software (<http://www.hyper.com/>). The pdbqt formats of the ligands were prepared by adding Gasteiger charges and setting the degree of torsions. The box dimensions were set to 60 × 60 × 60 with 0.375 Å grid spacing. In order to determine the docking parameter file, a rigid macromolecule was chosen. The Lamarckian genetic search algorithm was applied and the number of GA runs was set at 100. The other parameters were left at program default values. Finally, fifteen compounds were superimposed in the protein and the lowest docking binding energy conformation and theoretical Ki were visualized using AutoDock Tools 1.5.6 and the ligand-protein interactions pictures were created using discovery studio 2017 R2 client (<http://accelrys.com>).

#### Acknowledgement

We gratefully appreciate the Iran's National Science Foundation (INSF) and Shiraz University Research Councils for the financial support of this work.

#### Declaration of Competing Interest

The authors declare that they have no known competing financial interests or personal relationships that could have appeared to influence the work reported in this paper.

#### Appendix A. Supplementary material

Supplementary data to this article can be found online at <https://doi.org/10.1016/j.bmc.2020.115540>.

#### References

- Manganiello VC, Murata T, Taira M, Belfrage P, Degerman E. Diversity in cyclic nucleotide phosphodiesterase isoenzyme families. *Arch Biochem Biophys*. 1995;322:1–3.
- Manganiello VC, Taira M, Degerman E, Belfrage P. Type III cGMP-inhibited cyclic nucleotide phosphodiesterases (PDE 3 gene family). *Cell Signal*. 1995;7:445–455.
- Degerman E, Belfrage P, Manganiello VC. Structure, localization, and regulation of cGMP-inhibited phosphodiesterase (PDE3). *J Biol Chem*. 1997;272:6823–6826.
- Meacci E, Taira M, Moos M, et al. Molecular cloning and expression of human myocardial cGMP-inhibited cAMP phosphodiesterase. *PNAS*. 1992;89:3721–3725.
- Taira M, Hockman SC, Calvo JC, Belfrage P, Manganiello VC. Molecular cloning of the rat adipocyte hormone-sensitive cyclic GMP-inhibited cyclic nucleotide phosphodiesterase. *J Biol Chem*. 1993;268:18573–18579.
- Fisher DA, Smith JF, Pillar JS, Denis SH, Cheng JB. Isolation and characterization of PDE8A, a novel human cAMP-specific phosphodiesterase. *J. B. Cheng. Biochem Biophys Res Commun*. 1998;246(3):570–577.
- Hayashi M, Matsuhashima K, Ohashi H, et al. Molecular cloning and characterization of human PDE8B, a novel thyroid-specific isozyme of 3', 5'-cyclic nucleotide phosphodiesterase. *Biochem Biophys Res Commun*. 1998;250:751–756.
- Soderling SH, Bayuga SJ, Beavo JA. Cloning and characterization of a cAMP-specific cyclic nucleotide phosphodiesterase. *PNAS*. 1998;95:8991–8996.
- Fisher DA, Smith JF, Pillar JS, Denis SH, Cheng JB. Isolation and characterization of PDE9A, a novel human cGMP-specific phosphodiesterase. *J Biol Chem*. 1998;273:15559–15564.
- Fujishige K, Kotera J, Michibata H, et al. Cloning and characterization of a novel human phosphodiesterase that hydrolyzes both cAMP and cGMP (PDE10A). *J Biol Chem*. 1999;274:18438–18445.
- Fawcett L, Baxendale R, Stacey P, et al. Molecular cloning and characterization of a distinct human phosphodiesterase gene family: PDE11A. *PNAS*. 2000;97:3702–3707.
- Zhang L, Murray F, Zahno A, et al. Cyclic nucleotide phosphodiesterase profiling reveals increased expression of phosphodiesterase 7B in chronic lymphocytic leukemia. *PNAS*. 2008;105:19532–19537.
- Omori K, Kotera J. Overview of PDEs and their regulation. *Circ Res*. 2007;100:309–327.
- Savai R, Pullamsetti SS, Banat GA, et al. Targeting cancer with phosphodiesterase inhibitors. *Expert Opin Invest Drugs*. 2010;19:117–131.
- Shakur Y, Holst LS, Landstrom TR, Movsesian M, Degerman E, Manganiello V. Regulation and function of the cyclic nucleotide phosphodiesterase (PDE3) gene family. *Prog Nucleic Acid Res Mol Biol*. 2001;66:241–277.
- Soh JW, Mao Y, Kim MG, et al. Cyclic GMP mediates apoptosis induced by sulindac derivatives via activation of c-Jun NH2-terminal kinase 1. *Clin Cancer Res*. 2000;6:4136–4141.
- Cheng J, Grande JP. Cyclic nucleotide phosphodiesterase (PDE) inhibitors: novel therapeutic agents for progressive renal disease. *Exp Biol Med*. 2007;232:38–51.
- Murata T, Shimizu K, Narita M, Manganiello VC, Tagawa T. Characterization of phosphodiesterase 3 in human malignant melanoma cell line. *Anticancer Res*. 2002;22:3171–3174.
- Murata T, Sugatani T, Shimizu K, Manganiello VC, Tagawa T. Phosphodiesterase 3 as a potential target for therapy of malignant tumors in the submandibular gland. *Anticancer Drugs*. 2001;12:79–83.
- Moon E, Lee R, Near R, Weintraub L, Wolda S, Lerner A. Inhibition of PDE3B augments PDE4 inhibitor-induced apoptosis in a subset of patients with chronic lymphocytic leukemia. *Clin Cancer Res*. 2002;8:589–595.
- Palasz A, Cieź D. In search of uracil derivatives as bioactive agents. Uracils and fused uracils: Synthesis, biological activity and applications. *Eur J Med Chem*. 2015;97:582–611.
- Legraverend M, Grierson DS. The purines: Potent and versatile small molecule inhibitors and modulators of key biological targets. *Bioorg Med Chem*. 2006;14:3987–4006.
- Galmarini CM, Mackey JR, Dumontet C. Nucleoside analogues and nucleobases in cancer treatment. *Lancet Oncol*. 2002;3:415–424.
- Parker WB. Enzymology of purine and pyrimidine antimetabolites used in the treatment of cancer. *Chem Rev*. 2009;109:2880–2893.
- Calderón-Arancibia J, Espinosa-Bustos C, Cañete-Molina Á, et al. Synthesis and pharmacophore modelling of 2, 6, 9-trisubstituted purine derivatives and their potential role as apoptosis-inducing agents in cancer cell lines. *Molecules*. 2015;20:6808–6826.
- Kwon SU, Cho YJ, Koo JS, et al. Cilostazol prevents the progression of the symptomatic intracranial arterial stenosis: the multicenter double-blind placebo-controlled trial of cilostazol in symptomatic intracranial arterial stenosis. *Stroke*. 2005;36:782–786.
- Johnstone RA, Rose ME. A rapid, simple, and mild procedure for alkylation of phenols, alcohols, amides and acids. *Tetrahedron*. 1979;35:2169–2173.
- Rad MN, Khalafi-Nezhad A, Divar M, Behrouz S. Silica sulfuric acid (SSA) as a highly efficient heterogeneous catalyst for persilylation of purine and pyrimidine nucleobases and other N-heterocycles using HMDS. *Phosphorus Sulfur Silicon*. 2010;185:1943–1954.
- Demko ZP, Sharpless KB. Preparation of 5-substituted 1H-tetrazoles from nitriles in water. *J Org Chem*. 2001;66:7945–7950.
- Davari AS, Abnous K, Mehri S, Ghandadi M, Hadizadeh F. Synthesis and biological evaluation of novel pyridine derivatives as potential anticancer agents and phosphodiesterase-3 inhibitors. *Bioorg Chem*. 2014;57:83–89.
- Hadizadeh F, Moallem SA, Jaafari MR, et al. Synthesis and immunomodulation of human lymphocyte proliferation and cytokine (interferon-γ) production of four novel malonitrilamides. *Chem Biol Drug Des*. 2009;73668–73673.
- Tavakkol-Afshari J, Brook A, Mousavi SH. Study of cytotoxic and apoptogenic properties of saffron extract in human cancer cell lines. *Food Chem Toxicol*. 2008;46:3443–3447.